Study of the charged current meson production in Bjorken kinematics

Marat Siddikov, William Brooks
Departamento de Física, Universidad Técnica Federico Santa María,
y Centro Científico - Tecnológico de Valparaíso, Casilla 110-V, Valparaíso, Chile

We suggest to measure charged current meson production process, $ep \to \nu_e \pi^- p$, which might be used for extraction of the generalized parton distributions (GPDs)of the proton. This is a novel channel for study of GPDs, and in contrast to pion *photo*production, this process is sensitive to the unpolarized GPDs $H_{u,d}$, $E_{u,d}$. It has a very small contamination by higher twist and Bethe-Heitler type contributions. Since all produced hadrons are charged, we expect that the kinematics of this process could be reconstructed using missing mass techniques. We estimated the cross-sections in the kinematics of Jefferson Laboratory experiments and found that thanks to large luminosity the process can be measured with reasonable statistics. We demonstrated that the kinematics of the process might be fully reconstructed if 4-momenta of pion and scattered proton are known. We also discuss various photon-induced backgrounds (with undetected additional particles) and demonstrate that they might be eliminated with additional kinematic cuts which do not affect the cross-section of CCDVMP. This letter of intent is based on our recent publication Phys.Rev. D96 (2017) no.9, 096006.

I. INTRODUCTION

Understanding the structure of the hadrons presents a challenging problem both from the theoretical and experimental viewpoints. This structure is parametrized nowadays in terms of the so-called generalized parton distributions (GPDs), which can be studied in a wide class of processes [1, 2]. The early analysis were mostly based on experimental data on deeply virtual Compton scattering (DVCS) [3] and deeply virtual meson production (DVMP) [1, 2, 4–17], although it was soon realized that in view of the rich structure of GPDs, as well as from certain complications with GPD extraction from pion electroproduction [17–21], additional channels were needed. It was then suggested that GPDs might be accessed in ρ-meson photoproduction [22–26], timelike Compton Scattering [27–29], exclusive pion- or photon-induced lepton pair production [30, 31], and heavy charmonia photoproduction [32, 33] (gluon GPDs). The forthcoming results from the upgraded JLAB [17], COMPASS [34–39] as well as from J-PARC [31, 40], hopefully will enrich and enhance the early data from HERA and 6 GeV JLab experiments, as well as improve our understanding of the proton GPDs.

Recently we suggested that GPDs could be studied in neutrino-induced deeply virtual meson production (νDVMP) [41] of the pseudoscalar mesons (π, K, η), using the high-intensity NuMI beam at Fermilab [42]. The main advantage of this process is that contamination by twist-3 effects [43] is small, which implies that GPDs could be accessed at moderate virtualities Q^2, provided that the next-to-leading order (NLO) corrections are included [44]. In the Bjorken limit, neglecting the masses of pions and kaons, we may get information about a full flavor structure of GPDs. A suppression of Cabibbo forbidden, strangeness changing processes can be avoided if kaon production is accompanied by the conversion of a nucleon to strange baryons Λ and $\Sigma^{\pm,0}$; in such processes the transition GPDs are related by $SU(3)$ relations [45] to linear combinations of different flavor components of the nucleon GPDs. Recently it was suggested in [46–50] that this approach could be extended to D-meson production, a challenge for future high-energy neutrino experiments.

In this paper we extend our previous studies to the case of charged current meson (pion) production in electron-induced processes, such as *e.g.* $ep \to \nu_e \pi^- p$. The feasibility to study charged currents in JLAB kinematics has been demonstrated earlier in [51]. It is expected that after upgrade even higher luminosities up to $\mathcal{L} = 10^{38}\text{cm}^{-2} \cdot s^{-1}$ will be achieved [52], which implies that the DVMP cross-section could be measured with reasonable statistics. Since all produced hadrons are charged, the reconstruction of the kinematics of the process, despite of undetectability of neutrinos, should not present major difficulties. As will be shown below, the cross-section of this process on unpolarized targets is mostly sensitive to the GPDs H_u, H_d, providing important constraints on available parametrizations, as well as testing the GPD universality. Similar to the case of neutrino-production, this process has smaller contamination by higher twist effects compared to DVMP.

For the sake of brevity and conciseness, in this paper we do not consider other processes, where flavor multiplet partners of pions and protons are produced and which could be used to test other flavor combinations of GPDs [41].

The paper is organized as follows. In Section II we describe the framework used for the evaluation of pion production, taking into account NLO corrections. In Sections III and IV we review the contaminating corrections due to Bethe-Heitler mechanism and twist-three contributions, due to poorly known transversity GPDs. In Section V we present numerical results and make conclusions. Finally, in Section VI we discuss reconstruction of the kinematics of the

process, and overview additional cuts which should be introduced in order to eliminate backgrounds from photon-mediated processes.

II. CROSS-SECTION OF THE νDVMP PROCESS

The cross-section of pion production in charged current DVMP has a form

$$\frac{d\sigma}{dt\,dx_B dQ^2} = \Gamma \sum_{\nu\nu'} \mathcal{A}^*_{\nu',\nu L}\mathcal{A}_{\nu',\nu L}, \tag{1}$$

where $t = (p_2 - p_1)^2$ is the momentum transfer to the proton, $Q^2 = -q^2$ is the virtuality of the charged boson, $x_B = Q^2/(2p\cdot q)$ is the Bjorken variable, the subscript indices ν and ν' in the amplitude $\mathcal{A}$ refer to helicity states of the baryon before and after interaction, and the letter L reflects the fact that in the Bjorken limit the dominant contribution comes from the longitudinally polarized massive bosons $W^\pm$ [1, 2]. The kinematic factor Γ included in equation (1) is given explicitly, for the charged current case, by

$$\Gamma = \frac{G_F^2 f_M^2 x_B^2 \left(1 - y - \frac{\gamma^2 y^2}{4}\right)}{64\pi^3 Q^2 \left(1 + Q^2/M_W^2\right)^2 (1+\gamma^2)^{3/2}}, \tag{2}$$

where θ_W is the Weinberg angle, M_W is the mass of the heavy bosons $W^\pm$, G_F is the Fermi constant, f_π is the pion decay constant, and we used the shorthand notations

$$\gamma = \frac{2\,m_N x_B}{Q}, \quad y = \frac{Q^2}{s_{ep}\,x_B} = \frac{Q^2}{2m_N E_e\,x_B}. \tag{3}$$

where E_e is the electron energy in the target rest frame. In Bjorken kinematics, the amplitude $\mathcal{A}_{\nu',\nu L}$ factorizes into a convolution of hard and soft parts,

$$\mathcal{A}_{\nu',\nu} = \int_{-1}^{+1} dx \sum_{q=u,d,s,g} \sum_{\lambda\lambda'} \mathcal{H}^q_{\nu'\lambda',\nu\lambda}\mathcal{C}^q_{\lambda\lambda'}, \tag{4}$$

where x is the average light-cone fraction of the parton, the superscript q is its flavor, λ and λ' are the helicities of the initial and final partons, and $\mathcal{C}^q_{\lambda'\nu',\lambda\nu}$ is the hard coefficient function, which will be specified later. The soft matrix element $\mathcal{H}^q_{\nu'\lambda',\nu\lambda}$ in (6) is diagonal in quark helicities (λ, λ'), and for the twist-2 GPDs has the form,

$$\begin{aligned}\mathcal{H}^q_{\nu'\lambda',\nu\lambda} = \frac{2\delta_{\lambda\lambda'}}{\sqrt{1-\xi^2}} \Bigg(-g_A^q \begin{pmatrix} \left(1-\xi^2\right)H^q - \xi^2 E^q & \frac{(\Delta_1 + i\Delta_2)E^q}{2m} \\ -\frac{(\Delta_1 - i\Delta_2)E^q}{2m} & \left(1-\xi^2\right)H^q - \xi^2 E^q \end{pmatrix}_{\nu'\nu} \\ + \operatorname{sgn}(\lambda) g_V^q \begin{pmatrix} -\left(1-\xi^2\right)\tilde{H}^q + \xi^2\tilde{E}^q & \frac{(\Delta_1 + i\Delta_2)\xi\tilde{E}^q}{2m} \\ \frac{(\Delta_1 - i\Delta_2)\xi\tilde{E}^q}{2m} & \left(1-\xi^2\right)\tilde{H}^q - \xi^2\tilde{E}^q \end{pmatrix}_{\nu'\nu} \Bigg),\end{aligned} \tag{5}$$

where the constants g_V^q, g_A^q are the vector and axial current couplings to quarks, and the leading twist GPDs H^q, E^q, $\tilde{H}^q$ and $\tilde{E}^q$ are functions of the variables $\left(x, \xi, t, \mu_F^2\right)$, where the skewness ξ is related to the light-cone momenta of protons $p_{1,2}$ as $\xi = \left(p_1^+ - p_2^+\right)/\left(p_1^+ + p_2^+\right)$, the invariant momentum transfer is $t = \Delta^2 = (p_2 - p_1)^2$, and μ_F is the factorization scale (see e.g. [12, 15] for details of the kinematics). For the processes in which the baryonic state changes, e.g. $ep \to \nu_e \pi_0 n$, the transition GPDs can be linearly related via $SU(3)$ relations [45] to ordinary GPDs. For this reason, (4) may be effectively rewritten as

$$\mathcal{A}_{\nu',\nu} = \int_{-1}^{+1} dx \sum_{q=u,d,s} \sum_{\lambda} \mathcal{H}^q_{\nu'\lambda,\nu\lambda}\mathcal{C}^q_{\lambda}. \tag{6}$$

where $\mathcal{C}^q_\lambda$ is the diagonal term of the helicity matrix in the hard coefficient function. Its evaluation is quite straightforward, and in leading order over α_s it gets contributions from the diagrams shown schematically in Figure 1. In fact, it has been studied both for pion electroproduction [20, 21, 24, 53–56] and neutrinoproduction [41]. For the processes in which the baryon does not change its internal state, there are additional contributions from gluon GPDs, as shown

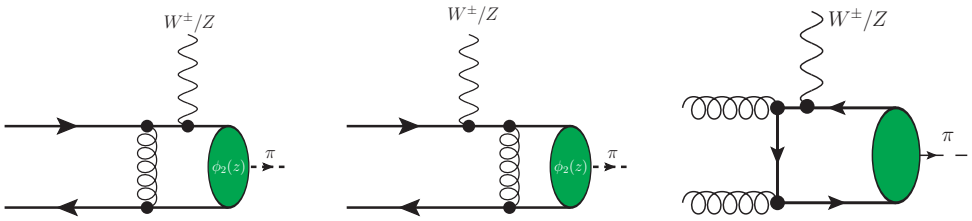

Figure 1: Leading-order contributions to the DVMP hard coefficient functions. Green blob stands for the pion wave function. Additional diagrams (not shown) may be obtained reversing the directions of the quark lines and in the case of the last diagram, permuting also the vector boson vertices.

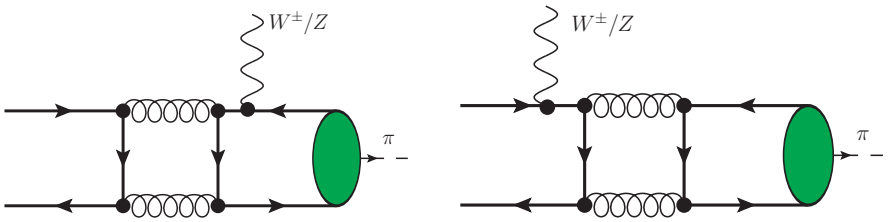

Figure 2: Sea quark contributions to the DVMP, which appear in the next-to-leading-order contributions. Additional diagrams (not shown) may be obtained by reversing the directions of the quark lines.

in the rightmost pane of Figure 1. These corrections are small for JLAB kinematics, yet give a contributions at higher energies. In next-to-leading order, the coefficient function includes an additional gluon attached in all possible ways to all diagrams in Figure 1, as well as additional contributions from sea quarks, as shown in Figure 2.

Straightforward evaluation of the diagrams shown in the Figures 1,2 yields for the coefficient functions

$$\mathcal{C}^q = \eta_-^q c_-^{(q)}(x,\,\xi) + \mathrm{sgn}(\lambda)\eta_+^q c_+^{(q)}(x,\,\xi) + \mathcal{O}\left(\frac{m^2}{Q^2}\right) + \mathcal{O}\left(\alpha_s^2\left(\mu_R^2\right)\right) \tag{7}$$

where the process-dependent flavor factors $\eta_{V\pm}^q$, $\eta_{A\pm}^q$ are given, for the case of pion production, in Table I [1]. In (7) we also introduced the shorthand notation

$$c_\pm^{(q)}(x,\xi) \;=\; \left(\int dz \frac{\phi_{2,\pi}(z)}{z}\right)\frac{8\pi i}{9}\frac{\alpha_s\left(\mu_R^2\right) f_M}{Q}\frac{1}{x\pm\xi\mp i0}\left(1+\frac{\alpha_s\left(\mu_r^2\right)}{2\pi}T^{(1)}\left(\frac{\xi\pm x}{2\xi},\,z\right)\right). \tag{8}$$

where $\phi_2(z)$ is the twist-2 $\pi-$or K-meson distribution amplitude (DA) [57]. The function $T^{(1)}(v,\,z)$ in (8) encodes NLO corrections to the coefficient function. As was explained in [58–60], it is related by analytical continuation to the loop correction to $\bar{q}q$ scattering, and was evaluated and analyzed in detail in the context of NLO studies of the

Table I: The flavor coefficients $\eta_\pm^q$, for several pion and kaon production processes discussed in this paper ($q = u, d, s, ...$). For the case of CC mediated processes, take $\eta_{V\pm}^q = \eta_\pm^q, \quad \eta_{A\pm}^q = -\eta_\pm^q$.

Process	η_+^q	η_-^q
$e\,p \to \nu_e \pi^- p$	$V_{ud}\delta_{qd}$	$V_{ud}\delta_{qu}$
$e\,p \to \nu_e \pi^0 n$	$V_{ud}\frac{\delta_{qu}-\delta_{qd}}{\sqrt{2}}$	$-V_{ud}\frac{\delta_{qu}-\delta_{qd}}{\sqrt{2}}$
$e\,p \to \nu_e K^- p$	$V_{us}\delta_{qs}$	$V_{us}\delta_{qs}$

Process	η_+^q	η_-^q
$e\,p \to \nu_e \pi^0 n$	$V_{ud}\frac{\delta_{qu}-\delta_{qd}}{\sqrt{2}}$	$-V_{ud}\frac{\delta_{qu}-\delta_{qd}}{\sqrt{2}}$
$e\,n \to \nu_e \pi^- n$	$V_{ud}\delta_{qu}$	$V_{ud}\delta_{qd}$
$e\,n \to \nu_e K^0 \Sigma^-$	0	$-V_{ud}\left(\delta_{qu}-\delta_{qs}\right)$

[1] As was discussed above, for processes with change of internal baryon structure, we use $SU(3)$ relations [45], which are valid up to corrections in current quark masses $\sim \mathcal{O}(m_q)$.

pion form factor (see [61, 62] for details and historical discussion). Explicitly, it is given by

$$
\begin{aligned}
T^{(1)}\left(v,\,z\right) = \frac{1}{2vz}\Bigg[& \frac{4}{3}\left(\left[3+\ln(v\,z)\right]\,\ln\left(\frac{Q^2}{\mu_F^2}\right)+\frac{1}{2}\ln^2\left(v\,z\right)+3\ln(v\,z)-\frac{\ln\bar{v}}{2\bar{v}}-\frac{\ln\bar{z}}{2\bar{z}}-\frac{14}{3}\right) \\
& +\beta_0\left(\frac{5}{3}-\ln(v\,z)-\ln\left(\frac{Q^2}{\mu_R^2}\right)\right) \\
& -\frac{1}{6}\left(2\frac{\bar{v}\,v^2+\bar{z}\,z^2}{(v-z)^3}\left[\mathrm{Li}_2(\bar{z})-\mathrm{Li}_2(\bar{v})+\mathrm{Li}_2(v)-\mathrm{Li}_2(z)+\ln\bar{v}\,\ln z-\ln\bar{z}\,\ln v\right]\right. \\
& +2\frac{v+z-2v\,z}{(v-z)^2}\ln\left(\bar{v}\bar{z}\right)+2\left[\mathrm{Li}_2(\bar{z})+\mathrm{Li}_2(\bar{v})-\mathrm{Li}_2(z)-\mathrm{Li}_2(v)+\ln\bar{v}\,\ln z+\ln\bar{z}\,\ln v\right] \\
& \left.+\,4\frac{v\,z\,\ln(v\,z)}{(v-z)^2}-4\ln\bar{v}\,\ln\bar{z}-\frac{20}{3}\right)\Bigg],
\end{aligned}
\tag{9}
$$

where $\beta_0=\frac{11}{3}N_c-\frac{2}{3}N_f$, $\mathrm{Li}_2(z)$ is the dilogarithm function, and μ_R and μ_F are the renormalization and factorization scales respectively. For processes when the internal state of the hadron is not changed, additional contributions come from the gluons and singlet (sea) quarks [58–60] [2],

$$
c^{(g)}\left(x,\xi\right) = \left(\int dz\frac{\phi_{2,\pi}\left(z\right)}{z\left(1-z\right)}\right)\frac{2\pi i}{3}\frac{\alpha_s\left(\mu_R^2\right)f_M}{Q}\frac{\xi}{\left(\xi+x-i0\right)\left(\xi-x-i0\right)}\left(1+\frac{\alpha_s\left(\mu_r^2\right)}{4\pi}\mathcal{I}^{(g)}\left(\frac{\xi-x}{2\xi},\,z\right)\right), \tag{10}
$$

$$
\begin{aligned}
\mathcal{I}^{(g)}\left(v,\,z\right) = & \left(\ln\left(\frac{Q^2}{\mu_F^2}\right)-1\right)\left[\frac{\beta_0}{2}+C_A\left[\left(1-v\right)^2+v^2\right]\left(\frac{\ln\left(1-v\right)}{v}+\frac{\ln v}{1-v}\right)-\frac{C_F}{2}\left(\frac{v\ln v}{1-v}+\frac{\left(1-v\right)\ln\left(1-v\right)}{v}\right)\right. \\
& \left.+\,C_F\left(\frac{3}{2}+2\,z\ln\left(1-z\right)\right)\right]-2\,C_F-\frac{\beta_0}{2}\left(\ln\left(\frac{Q^2}{\mu_R^2}\right)-1\right)-\frac{C_F\left(1-2\,v\right)}{2\,\left(z-v\right)}R\left(z,\,v\right) \\
& +\frac{\left(2C_A-C_F\right)}{4}\left(\frac{v\,\ln^2 v}{1-v}+\frac{\left(1-v\right)\ln^2\left(1-v\right)}{v}\right)+C_F(1+3\,z)\ln\left(1-z\right)+ \\
& +\left(\ln\,v+\ln\left(1-v\right)\right)\left[C_F\left(1-z\right)\ln\,z-\frac{1}{4}+2C_F-C_A\right] \\
& +\frac{C_A}{2}\left(\ln\left(z\left(1-z\right)\right)-2\right)\left[\frac{v\,\ln v}{1-v}+\frac{\left(1-v\right)\,\ln\left(1-v\right)}{v}\right] \\
& +C_F z\,\ln^2\left(1-z\right)+\frac{C_A}{2}\left(1-2\,v\right)\ln\left(\frac{v}{1-v}\right)\left[\frac{3}{2}+\ln\left(z\,\left(1-z\right)\right)+\ln\left(v\,\left(1-v\right)\right)\right] \\
& +\left(C_F\left(\left(z-v\right)^2-v\left(1-v\right)\right)-\left(C_F-\frac{C_A}{2}\right)\left(z-v\right)(1-2v)\right)\times \\
& \times\left[-\frac{R(z,v)}{(z-v)^2}+\frac{\ln v+\ln z-\ln\left(1-v\right)-\ln\left(1-z\right)}{2\left(z-v\right)}+\frac{(z-v)^2-v(1-v)}{(z-v)^3}H(z,v)\right] \\
& +\Big\{\,z\to 1-z\Big\},
\end{aligned}
\tag{11}
$$

$$
C_F = \frac{N_c^2-1}{2N_c},\quad C_A=N_c. \tag{12}
$$

---

[2] For the sake of simplicity, we follow [60] and assume that the factorization scale μ_F is the same for both the generalized parton distribution and the pion distribution amplitude.

$$c_{\pm}^{(s)}(x,\xi) = -\left(\int dz \frac{\phi_{2,\pi}(z)}{z(1-z)}\right) \frac{4i\alpha_s^2\left(\mu_R^2\right) f_M}{9\,Q} \mathcal{I}^{(s)}\left(\frac{x\pm\xi}{2\xi}, z\right), \tag{13}$$

$$\mathcal{I}^{(s)}(v,z) = (1-2\,v)\left(\frac{\ln v}{1-v} + \frac{\ln(1-v)}{v}\right)\ln\left(\frac{Q^2 z}{\mu_F^2}\right) + \frac{1-2v}{2}\left[\frac{\ln^2 v}{1-v} + \frac{\ln^2(1-v)}{v}\right] \tag{14}$$

$$-\frac{R(v,z)}{z-v} - \frac{(1-v)\ln(1-v) - v\ln v}{v(1-v)} + \frac{(z-v)^2 - v(1-v)}{(z-v)^2} H(v,z) + \Big\{ z \to 1-z \Big\},$$

$$R(v,z) = z\ln v + (1-z)\ln(1-v) + z\ln z + (1-v)\ln(1-v), \tag{15}$$

$$H(v,z) = \mathrm{Li}_2(1-v) - \mathrm{Li}_2(v) + \mathrm{Li}_2(z) - \mathrm{Li}_2(1-z) + \ln v \ln(1-z) - \ln(1-v)\ln z. \tag{16}$$

Some coefficient functions have non-analytic behavior $\sim \ln^2 v$ for small $v \approx 0$ ($x = \pm\xi \mp i0$), which signals that a collinear approximation might be not valid near this point. This singularity in the collinear limit occurs due to the omission of the small transverse momentum $l_{M,\perp}$ of the quark inside a meson [19], and for this reason the contribution of the region $|v| \sim l_{M,\perp}^2/Q^2$ should be treated with due care for finite Q^2 (beyond the Bjorken limit). Moreover, a full evaluation of $T^{(1)}(v,z)$ beyond the collinear approximation (taking into account all higher twist corrections) presents a challenging problem and has not been done so far. It was observed in [60], that the singular terms might be eliminated by a redefinition of the renormalization scale μ_R; however, near the point $v \approx 0$ the scale μ_R^2 becomes soft, $\mu_R^2 \sim z\,v\,Q^2 \lesssim l_\perp^2$, which is another manifestation that nonperturbative effects become relevant. For this reason, sufficiently large value of Q^2 should be used to mitigate contributions of higher twist effects. As we will see below, for $Q^2 \approx 4$ GeV^2 the contribution of this soft region is small, so the collinear factorization is reliable.

III. BETHE-HEITLER TYPE CONTRIBUTION

As was found in Ref. [63], in the asymptotic Bjorken limit ($Q^2 \to \infty$) the DVMP contribution gets overwhelmed by subleading $\mathcal{O}(\alpha_{em})$ Bethe-Heitler type (BH) contributions, shown in Figure 3. These diagrams have milder suppression at large Q^2 compared to DVMP and are additionally enhanced by the t-channel photon pole $\sim 1/t$ in the forward kinematics, and for this reason at sufficiently large $\sim Q^2/t$ this mechanism becomes dominant[3].

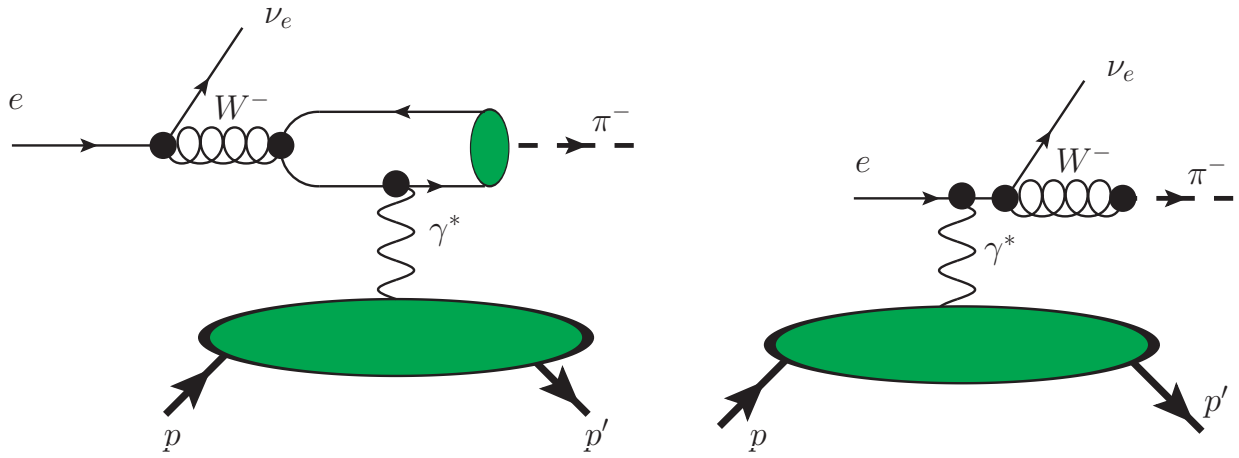

Figure 3: Bethe-Heitler contribution in the charged current DVMP. Formally it is suppressed as $\mathcal{O}(\alpha_{\rm em})$ compared to DVMP contribution; however, for the asymptotic Bjorken limit it becomes the dominant mechanism due to relative enhancement by a kinematical factor $\sim Q^2/t\,\alpha_s(Q^2)$. The green blob stands for the pion wave function.

While for the DVMP amplitude evaluation presented in the previous section the dominant contribution comes from the longitudinally polarized mediator boson, for the BH this is no longer true and we have to consider all the W polarizations. The left diagram in Figure 3 contains the matrix element

[3] As was estimated in [63], the cross-section of Bethe-Heitler mechanism becomes comparable to DVMP for $Q^2 \gtrsim 100$ GeV^2

$$\mathcal{A}^{ab}_{\mu\nu}\left(q,\Delta\right)=\frac{1}{f_\pi}\int d^4x\, e^{-iq\cdot x}\left\langle 0\left|\left(V^a_\mu(x)-A^a_\mu(x)\right)J^{em}_\nu(0)\right|\pi^b\left(q-\Delta\right)\right\rangle, \tag{17}$$

where $V^a_\mu(x)$ and $A^a_\mu(x)$ are the vector and axial isovector currents. We evaluate the correlator (17) perturbatively in the collinear approximation, which is justified by the intermediate boson large Q^2 value, and therefore consider only the dominant contribution from the leading twist-2 pion DA. The evaluation details may be found in [63], while here for the sake of brevity we will only provide the final result. The cross-section of the Bethe-Heitler mechanism is given by

$$\frac{d^4\sigma^{(BH)}}{dt\,d\ln x_{Bj}\,dQ^2d\varphi}=\frac{f_\pi^2G_F^2\alpha_{em}^2\sum_{n=0}^{2}\mathcal{C}_n^{BH}\cos(n\varphi)}{16\,\pi^2t^2\left(1+\frac{4m_N^2x_B^2}{Q^2}\right)^{5/2}}, \tag{18}$$

where φ is the angle between the lepton scattering and the pion production planes, and in addition to the kinematic variables defined in the previous section II we introduced shorthand notations

$$\begin{aligned}
\mathcal{C}_0^{BH}=&\,\mathcal{C}_2^{BH}+\frac{m_N^2}{9\,Q^2}\Big[4\left(\left(2y^2+y-1\right)\left(\phi_{-1}-1\right)x_B^3\right. \\
&-\left(\left(4\left(\phi_{-1}-1\right)^2+\frac{t}{2m_N^2}\left(4\phi_{-1}^2-8\phi_{-1}+5\right)\right)y^2-4\left(\left(\phi_{-1}-1\right)^2+\frac{t}{4m_N^2}\left(4\phi_{-1}^2-13\phi_{-1}+10\right)\right)y\right. \\
&\left.+\frac{5t}{2m_N^2}\left(\phi_{-1}-2\right)^2+\left(\phi_{-1}-1\right)^2\right)x_B^2+\left(2y-1\right)\frac{t}{m_N^2}\left(\phi_{-1}-1\right)\left(-\phi_{-1}+y\left(2\phi_{-1}-1\right)+2\right)x_B \\
&-4\left(1-2y\right)^2\frac{t}{4m_N^2}\left(\phi_{-1}-1\right)^2\Big)F_1^2(t)+2F_1(t)F_2(t)x_B^2\left(x_B^2\left(y+1\right)^2-\frac{x_Bt}{m_N^2}\left(y+1\right)^2\right. \\
&\left.-\frac{t}{m_N^2}\left(\left(8\phi_{-1}^2-24\phi_{-1}+17\right)y^2-2\left(8\phi_{-1}^2-24\phi_{-1}+19\right)y+10\phi_{-1}^2-36\phi_{-1}+35\right)\right) \\
&+F_2^2\left(\left(y+1\right)^2\left(\frac{t}{4m_N^2}+1\right)x_B^4-\left(y+1\right)\frac{t}{m_N^2}\left(\frac{t}{4m_N^2}-\phi_{-1}+y\left(\frac{t}{4m_N^2}+2\phi_{-1}-1\right)+2\right)x_B^3\right. \\
&+\frac{t\,x_B^2}{m_N^2}\left(\left(-4\phi_{-1}^2+16\phi_{-1}+\frac{t}{4m_N^2}\left(8\phi_{-1}-7\right)-13\right)y^2\right. \\
&\left.+2\left(6\phi_{-1}^2-20\phi_{-1}+\frac{t}{4m_N^2}\left(2\phi_{-1}-1\right)+17\right)y-9\phi_{-1}^2+\frac{t}{4m_N^2}\left(5-4\phi_{-1}\right)+34\phi_{-1}-34\right) \\
&\left.-\left(2y-1\right)\left(\frac{t}{m_N^2}\right)^2\left(\phi_{-1}-1\right)\left(-\phi_{-1}+y\left(2\phi_{-1}-1\right)+2\right)x_B+\left(1-2y\right)^2\left(\frac{t}{4m_N^2}\right)^2\left(\phi_{-1}-1\right)^2\right)\Big] \\
&+\mathcal{O}\left(\frac{m_N^4}{Q^4},\frac{t^2}{Q^4}\right),
\end{aligned} \tag{19}$$

$$\mathcal{C}_1^{BH} = \frac{K\,m_N^2}{9Q^2}\,\Big[4\left(3\left(-4y+3\left(y-2\right)\phi_{-1}+9\right)x_B^3\right. \tag{20}$$
$$-2\left(\phi_{-1}-1\right)\left(-\left(\frac{5t}{2m_N^2}+9\right)\phi_{-1}+2y\left(\frac{t\phi_{-1}}{m_N^2}-\frac{3t}{4m_N^2}+3\phi_{-1}-6\right)+18\right)x_B^2$$
$$+\left.\frac{3t}{m_N^2}\left(\phi_{-1}-1\right)\left(-6\phi_{-1}+y\left(4\phi_{-1}-3\right)+3\right)x_B-\left(2y-3\right)\frac{6\,t}{m_N^2}\left(\phi_{-1}-1\right)^2\right)F_1^2(t)$$
$$+4F_1(t)F_2(t)x_B^2\left(3\left(y-3\right)x_B^2-12\left(y-3\right)\frac{t}{4m_N^2}x_B-8\frac{t}{4m_N^2}\left(4y\left(\phi_{-1}-3\right)-5\phi_{-1}+18\right)\left(\phi_{-1}-1\right)\right)$$
$$-F_2^2(t)\left(-6\left(y-3\right)x_B^4\right.$$
$$+\frac{t}{4m_N^2}\left(-6\left(y-3\right)x_B^2+12\left(-2y+3\left(y-2\right)\phi_{-1}+3\right)x_B+8\left(2y\left(\phi_{-1}-6\right)-\phi_{-1}+18\right)\left(\phi_{-1}-1\right)\right)x_B^2$$
$$\left.+24\left(\frac{t}{4m_N^2}\right)^2\left(x_B\left(x_B-2\phi_{-1}+2\right)+2\left(\phi_{-1}-1\right)\right)\left(x_B\left(y-3\right)-2\left(2y-3\right)\left(\phi_{-1}-1\right)\right)\right)\Big]$$
$$+\mathcal{O}\left(\frac{m_N^4}{Q^4},\frac{t^2}{Q^4}\right)$$

$$\mathcal{C}_2^{BH} = -\frac{4\,K^2}{9}\left[\left(5x_B-4\phi_{-1}+4\right)\left(\phi_{-1}-1\right)F_1^2(t)+2x_B^2F_1(t)F_2(t)\right. \tag{21}$$
$$\left.+\left(\left(1+\frac{t}{4m_N^2}\right)x_B^2-\frac{5\,t\,x_B}{4m_N^2}\left(\phi_{-1}-1\right)+\frac{t}{m_N^2}\left(\phi_{-1}-1\right)^2\right)F_2^2(t)\right]$$
$$+\mathcal{O}\left(\frac{m_N^2}{Q^2},\frac{t}{Q^2}\right),$$

$$K^2 = \frac{\Delta_\perp^2}{Q^2}\left(1-y-\frac{y^2\epsilon^2}{4}\right) \tag{22}$$
$$= -\frac{t}{Q^2}\left(1-x_B\right)\left(1-y-\frac{\epsilon^2y^2}{4}\right)\left(1-\frac{t_{min}}{t}\right)\left\{\sqrt{1+\epsilon^2}+\frac{4x_B\left(1-x_B\right)+\epsilon^2}{4\left(1-x_B\right)}\frac{t-t_{min}}{Q^2}\right\},$$
$$\epsilon^2 = \frac{4m_N^2x_B^2}{Q^2},\quad t_{min} = -\frac{m_N^2x_B^2}{1-x_B}+\mathcal{O}\left(\frac{m_N^2}{Q^2},\frac{t}{Q^2}\right),\qquad \phi_{-1} = \int_0^1\frac{\phi_{2,\pi}(z)}{z}\,dz. \tag{23}$$

In the expressions (19-21) we use the notation $F_{1,2}(t)$ for the Dirac and Pauli form factors. As we can see, the BH cross-section is symmetric under the $\varphi\to-\varphi$ transformation. For asymptotically large Q^2, the $\mathcal{C}_1^{BH}$ harmonic is suppressed by $\Delta_\perp/Q$, whereas $\mathcal{C}_0^{BH}\sim\mathcal{C}_2^{BH}$, and therefore the distribution is also symmetric with respect to the $\varphi\to\pi-\varphi$ transformation.

The interference between the DVMP and BH amplitudes yields an additional contribution

$$\frac{d^4\sigma^{(int)}}{dt\,d\ln x_{Bj}\,dQ^2d\varphi} = \frac{f_\pi^2G_F^2\,x_B\alpha_{em}\alpha_S\phi_{-1}\left(\mathcal{C}_0^{int}+\mathcal{C}_1^{int}\cos\varphi+\mathcal{S}_1^{int}\sin\varphi\right)}{36\,\pi^2t\,Q^2\left(1-\frac{x_B}{2}\right)\left(1+\frac{4m_N^2x_B^2}{Q^2}\right)^{5/2}}, \tag{24}$$

where

$$\mathcal{C}_0^{int} = -\frac{m_N^2(1-y)}{Q^2}\left(\left(-4\left(1-x_B\right)\Re e\mathcal{H} + x_B^2\,\Re e\mathcal{E}\right)F_1 + \Re e\mathcal{E}\,F_2\frac{t}{4m_N^2}(x_B-2)^2 + \left(\Re e\mathcal{H}+\Re e\mathcal{E}\right)F_2 x_B^2\right) \tag{25}$$
$$\times\left(\left(2\phi_{-1}-3\right)x_B^2 - \frac{t}{m_N^2}\left(\phi_{-1}-1\right)\left(1+x_B\right)\right) + \mathcal{O}\left(\frac{m_N^2}{Q^2},\frac{t}{Q^2}\right),$$

$$\mathcal{C}_1^{int} = \frac{K}{3}\left[F_1\left(2\,\mathcal{R}e\,\mathcal{E}\left(y-3\right)x_B^2 + \mathcal{R}e\,\mathcal{H}\left(4\left(x_B-2\right)\left(2y-3\right)\phi_{-1} - 4\left(\left(x_B-4\right)y+6\right)\right)\right)\right. \tag{26}$$
$$+ F_2\left(2\,\mathcal{R}e\mathcal{H}\left(y-3\right)x_B^2 + \mathcal{R}e\,\mathcal{E}\left(2x_B^2\left(y-3\right) - \left(x_B-2\right)\frac{t}{4m_N^2}\left(4\left(2y-3\right)\left(\phi_{-1}-1\right) - 2x_B\left(y-3\right)\right)\right)\right)$$
$$\left. + \mathcal{O}\left(\frac{m_N^2}{Q^2},\frac{t}{Q^2}\right)\right]$$

$$\mathcal{S}_1^{int} = \frac{K\left(2-x_B\right)}{6}\left[F_1\left(-2\,\mathcal{I}m\,\mathcal{E}\left(y+1\right)x_B^2 - 2\,\mathcal{I}m\,\mathcal{H}\left(x_B\left(4\phi_{-1}y - 2y - 2\phi_{-1}+4\right) - 4\left(2y-1\right)\left(\phi_{-1}-1\right)\right)\right)\right. \tag{27}$$
$$+ F_2\left(-2\,\mathcal{I}m\,\mathcal{H}\left(y+1\right)x_B^2\right.$$
$$\left.\left. -2\,\mathcal{I}m\,\mathcal{E}\left(\left(y+1\right)\left(1+\frac{t}{4m_N^2}\right)x_B^2 + \frac{t}{2m_N^2}\left(-2\phi_{-1}y + y + \phi_{-1} - 2\right)x_B + \left(2y-1\right)\frac{t}{m_N^2}\left(\phi_{-1}-1\right)\right)\right)\right.$$
$$\left. + \mathcal{O}\left(\frac{m_N^2}{Q^2},\frac{t}{Q^2}\right)\right],$$

The angular dependence of the interference term (24) has a $\sim \sin\varphi$ term, which stems from the interference of the vector and axial vector currents in the lepton part of the diagram. This interference contribution depends only linearly on the target GPDs and for this reason presents interesting opportunities for studies at future colliders.

As we will see below, in JLAB kinematics the contribution of both BH and interference terms are small, and for this reason it is convenient to assess their size in terms of the angular harmonics c_n, s_n, normalizing the total cross-section to the cross-section of the dominant DVMP process as[4]

$$\frac{d^4\sigma^{(tot)}}{dt\,d\ln x_{Bj}\,dQ^2 d\varphi} = \frac{1}{2\pi}\frac{d^4\sigma^{(DVMP)}}{dt\,d\ln x_{Bj}\,dQ^2}\left(1 + \sum_{n=0}^{2} c_n\cos(n\varphi) + s_1\sin(\varphi)\right). \tag{28}$$

IV. TWIST-THREE CORRECTIONS

In the Bjorken limit, the dominant contribution comes from the twist-two GPDs H, E, $\tilde{H}$, $\tilde{E}$. However, in modern experiments a large part of the data comes from the region of Q only two or three times larger than the nucleon mass m_N. For this reason it is important to assess how large are the omitted higher-twist contributions. Previously this analysis was done by us in the context of neutrino-production [43], and here we repeat it for the case of charged current meson production.

The additional contribution to the amplitude (5) from transversity GPDs is given by

$$\delta\mathcal{H}^q_{\nu'\lambda',\nu\lambda} = \left(m^q_{\nu'\nu}\delta_{\lambda,-}\delta_{\lambda',+} + n^q_{\nu'\nu}\delta_{\lambda,+}\delta_{\lambda',-}\right), \tag{29}$$

---

[4] Compared to our earlier [63], we modified the definition of c_0 and explicitly took out the unit term in (28), in order to have uniform counting c_n, $s_n \sim \mathcal{O}\left(\alpha_{\rm em}\right)$ for all harmonics.

where the coefficients $m^q_{\pm,\pm}$ and $n^q_{\pm,\pm}$ are linear combinations of the transversity GPDs,

$$m^q_{--} = \frac{\sqrt{-t'}}{4m}\left[2\tilde{H}^q_T + (1+\xi)E^q_T - (1+\xi)\tilde{E}^q_T\right], \tag{30}$$

$$m^q_{-+} = \sqrt{1-\xi^2}\frac{t'}{4m^2}\tilde{H}^q_T, \tag{31}$$

$$m^q_{+-} = \sqrt{1-\xi^2}\left[H^q_T - \frac{\xi^2}{1-\xi^2}E^q_T + \frac{\xi}{1-\xi^2}\tilde{E}^q_T - \frac{t'}{4m^2}\tilde{H}^q_T\right], \tag{32}$$

$$m^q_{++} = \frac{\sqrt{-t'}}{4m}\left[2\tilde{H}^q_T + (1-\xi)E^q_T + (1-\xi)\tilde{E}^q_T\right], \tag{33}$$

$$n^q_{--} = -\frac{\sqrt{-t'}}{4m}\left(2\tilde{H}^q_T + (1-\xi)E^q_T + (1-\xi)\tilde{E}^q_T\right), \tag{34}$$

$$n^q_{-+} = \sqrt{1-\xi^2}\left(H^q_T - \frac{\xi^2}{1-\xi^2}E^q_T + \frac{\xi}{1-\xi^2}\tilde{E}^q_T - \frac{t'}{4m^2}\tilde{H}^q_T\right), \tag{35}$$

$$n^q_{+-} = \sqrt{1-\xi^2}\frac{t'}{4m^2}\tilde{H}^q_T, \tag{36}$$

$$n^q_{++} = -\frac{\sqrt{-t'}}{4m}\left(2\tilde{H}^q_T + (1+\xi)E^q_T - (1+\xi)\tilde{E}^q_T\right), \tag{37}$$

and we introduced a shorthand notation $t' = -\Delta^2_\perp/(1-\xi^2)$; $\Delta_\perp = p_{2,\perp} - p_{1,\perp}$ is the transverse part of the momentum transfer. The coefficient function (7) gets an additional nondiagonal in parton helicity contribution,

$$\delta\mathcal{C}^q_{\lambda' 0,\lambda\mu} == \delta_{\mu,+}\delta_{\lambda,-}\delta_{\lambda',+}\left(S^q_A - S^q_V\right) + \delta_{\mu,-}\delta_{\lambda,+}\delta_{\lambda',-}\left(S^q_A + S^q_V\right) + \mathcal{O}\left(\frac{m^2}{Q^2}\right), \tag{38}$$

where we introduced the shorthand notations

$$S^q_A = \int dz\left(\left(\eta^q_{A+}c^{(3,p)}_+(x,\xi) - \eta^q_{A-}c^{(3,p)}_-(x,\xi)\right) + 2\left(\eta^q_{A-}c^{(3,\sigma)}_-(x,\xi) + \eta^q_{A+}c^{(3,\sigma)}_+(x,\xi)\right)\right), \tag{39}$$

$$S^q_V = \int dz\left(\left(\eta^q_{V+}c^{(3,p)}_+(x,\xi) + \eta^q_{V-}c^{(3,p)}_-(x,\xi)\right) + 2\left(\eta^q_{V+}c^{(3,\sigma)}_+(x,\xi) - \eta^q_{V-}c^{(3,\sigma)}_-(x,\xi)\right)\right), \tag{40}$$

$$c^{(3,i)}_+(x,\xi) = \frac{4\pi i\alpha_s f_\pi\xi}{9\,Q^2}\int_0^1 dz\frac{\phi_{3,i}(z)}{z(x+\xi)^2}, \quad c^{(3,i)}_-(x,\xi) = \frac{4\pi i\alpha_s f_\pi\xi}{9\,Q^2}\int_0^1 dz\frac{\phi_{3,i}(z)}{(1-z)(x-\xi)^2}; \tag{41}$$

and the twist-three pion distributions are defined as

$$\phi^{(p)}_3(z) = \frac{1}{f_\pi\sqrt{2}}\frac{m_u+m_d}{m^2_\pi}\int\frac{du}{2\pi}e^{i(z-0.5)u}\left\langle 0\left|\bar{\psi}\left(-\frac{u}{2}n\right)\gamma_5\psi\left(\frac{u}{2}n\right)\right|\pi(q)\right\rangle, \tag{42}$$

$$\phi^{(\sigma)}_3(z) = \frac{3i}{\sqrt{2}f_\pi}\frac{m_u+m_d}{m^2_\pi}\int\frac{du}{2\pi}e^{i(z-0.5)u}\left\langle 0\left|\bar{\psi}\left(-\frac{u}{2}n\right)\sigma_{+-}\gamma_5\psi\left(\frac{u}{2}n\right)\right|\pi(q)\right\rangle. \tag{43}$$

Thanks to symmetry of ϕ_p and antisymmetry of ϕ_σ with respect to charge conjugation, the dependence on the pion DAs factorizes in the collinear approximation and contributes only as the minus one first moment of the linear combination of the twist-3 DAs, $\phi_p(z) + 2\phi_\sigma(z)$,

$$\left\langle\phi^{-1}_3\right\rangle = \int_0^1 dz\frac{\phi^{(p)}_3(z) + 2\phi^{(\sigma)}_3(z)}{z}. \tag{44}$$

In the general case the coefficient function (41) leads to collinear divergencies near the points $x = \pm\xi$, when substituted to (6). As was noted in [19], this singularity is naturally regularized by the the small transverse momentum of the

quarks inside the meson. Such regularization modifies (41) to

$$c_+^{(3,i)}(x,\xi) = \frac{4\pi i\alpha_s f_\pi \xi}{9\,Q^2}\int_0^1 dz\, d^2 l_\perp \frac{\phi_{3,i}(z,\, l_\perp)}{(x+\xi-i0)\left(z(x+\xi)+\frac{2\xi\, l_\perp^2}{Q^2}\right)}, \tag{45}$$

$$c_-^{(3,i)}(x,\xi) = \frac{4\pi i\alpha_s f_\pi \xi}{9\,Q^2}\int_0^1 dz\, d^2 l_\perp \frac{\phi_{3,i}(z,\, l_\perp)}{(x-\xi+i0)\left((1-z)(x-\xi)-\frac{2\xi\, l_\perp^2}{Q^2}\right)}, \tag{46}$$

where $l_\perp$ is the transverse momentum of the quark, and we tacitly assume absence of any other transverse momenta in the coefficient function. Due to interference of the leading twist and twist-there contributions, the total cross-section acquires dependence on the angle φ between lepton scattering and pion production planes,

$$\begin{aligned}\frac{d\sigma}{dt\,dx_B dQ^2 d\varphi} &= \epsilon\frac{d\sigma_L}{dt\,dx_B dQ^2 d\varphi} + \frac{d\sigma_T}{dt\,dx_B dQ^2 d\varphi} + \sqrt{\epsilon(1+\epsilon)}\cos\varphi\frac{d\sigma_{LT}}{dt\,dx_B dQ^2 d\varphi} \\ &+ \epsilon\cos(2\varphi)\,\frac{d\sigma_{TT}}{dt\,dx_B dQ^2 d\varphi} + \sqrt{\epsilon(1+\epsilon)}\sin\varphi\frac{d\sigma_{L'T}}{dt\,dx_B dQ^2 d\varphi} + \epsilon\sin(2\varphi)\,\frac{d\sigma_{T'T}}{dt\,dx_B dQ^2 d\varphi},\end{aligned} \tag{47}$$

where we introduced the shorthand notations

$$\epsilon = \frac{1-y-\frac{\gamma^2 y^2}{4}}{1-y+\frac{y^2}{2}+\frac{\gamma^2 y^2}{4}}.$$

$$\frac{d\sigma_L}{dt\,dx_B dQ^2 d\varphi} = \frac{\Gamma\,\sigma_{00}}{2\pi\epsilon} \tag{48}$$

$$\frac{d\sigma_T}{dt\,dx_B dQ^2 d\varphi} = \frac{\Gamma}{2\pi\epsilon}\left(\frac{\sigma_{++}+\sigma_{--}}{2}+\frac{1}{2}\sqrt{1-\epsilon^2}\frac{\sigma_{++}-\sigma_{--}}{2}\right) \tag{49}$$

$$\frac{d\sigma_{LT}}{dt\,dx_B dQ^2 d\varphi} = \frac{\Gamma}{2\pi\epsilon}\left(\mathrm{Re}\,(\sigma_{0+}-\sigma_{0-})+\frac{1}{2}\sqrt{\frac{1-\epsilon}{1+\epsilon}}\mathrm{Re}\,(\sigma_{0+}+\sigma_{0-})\right) \tag{50}$$

$$\frac{d\sigma_{TT}}{dt\,dx_B dQ^2 d\varphi} = -\frac{\Gamma}{2\pi\epsilon}\,\mathrm{Re}\,(\sigma_{+-}) \tag{51}$$

$$\frac{d\sigma_{L'T}}{dt\,dx_B dQ^2 d\varphi} = -\frac{\Gamma}{2\pi\epsilon}\left(\mathrm{Im}\,(\sigma_{+0}+\sigma_{-0})-\frac{1}{2}\sqrt{\frac{1-\epsilon}{1+\epsilon}}\mathrm{Im}\,(\sigma_{-0}-\sigma_{+0})\right) \tag{52}$$

$$\frac{d\sigma_{T'T}}{dt\,dx_B dQ^2 d\varphi} = -\frac{\Gamma}{2\pi\epsilon}\,\mathrm{Im}\,(\sigma_{+-}) \tag{53}$$

and the subindices α, β in

$$\sigma_{\alpha\beta} = \sum_{\nu\nu'}\mathcal{A}^*_{\nu' 0,\nu\alpha}\mathcal{A}_{\nu' 0,\nu\beta},$$

refer to polarizations of intermediate heavy boson in the amplitude and its conjugate. As we will see below, in JLAB kinematics the contribution of higher twist corrections is small, and for this reason, similar to the Bethe-Heitler case, we will quantify their size in terms of the angular harmonics c_n, s_n, normalizing the total cross-section to the cross-section of the dominant DVMP process as defined in (28).

V. RESULTS AND DISCUSSION

In this section we would like to present the numerical results for the charged current pion production . For the sake of definiteness, for numerical estimates we use the Kroll-Goloskokov parametrization of GPDs [19, 20, 54–56], and assume the asymptotic form of the pion wave function, $\phi_2(z) = 6\,z\,(1-z)$. For estimates of the twist-3 contribution introduced in Section II, we use the parametrization suggested in [19, 20],

$$\phi_3(z,\, l_\perp) = \phi_{3;p}(z,\, l_\perp) + 2\phi_{3;\sigma}(z,\, l_\perp) = \frac{2a_p^3}{\pi^{3/2}} l_\perp \phi_{as}(z)\exp\left(-a_p^2 l_\perp^2\right). \tag{54}$$

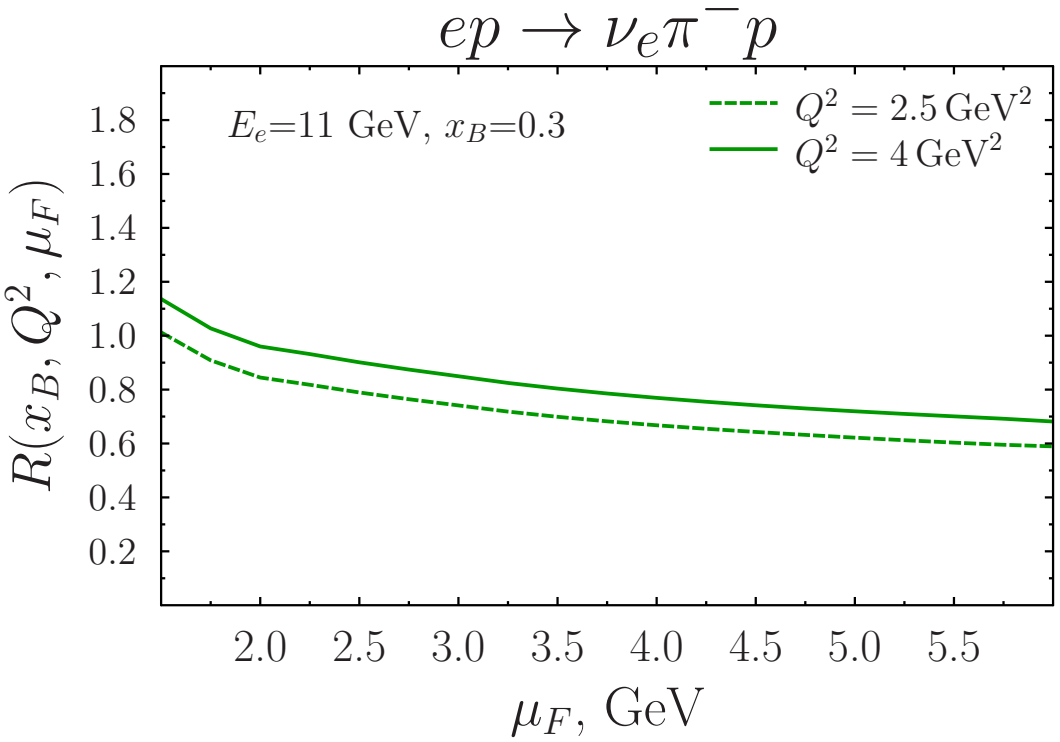

Figure 4: (color online) Factorization scale dependence of the charged current process $ep \to \nu_e \pi^- p$. The ratio R is defined as $R\left(x_B,\, Q^2,\, \mu_F\right) = d\sigma\left(x_B,\, Q^2,\, \mu_F\right)/d\sigma\left(x_B,\, Q^2,\, \mu_F = Q\right)$. A similar dependence is observed for all other processes.

where the numerical constant a_p is taken as $a_p \approx 2\,\mathrm{GeV}^{-1}$.

We would like to start with a discussion of the dependence on the factorization scale μ_F, which separates hard and soft physics. As we can see from Figure 4, the dependence on the factorization scale μ_F is mild and disappears for $\mu_F \gtrsim 5$ GeV. Though the choice of factorization scale μ_F is arbitrary, taking its value significantly different from the virtuality Q would lead to large logarithms in higher order corrections. As was suggested in [58–60], varying the scale in the range $\mu_F \in (Q/2,\, 2Q)$, we can roughly estimate the error due to omitted higher order loop contributions.

In Figure 5 we show the predictions for the differential cross-section $d\sigma/dx_B\, dQ^2$ for charged pion production for two virtualities Q^2. At fixed electron energy E_e and virtuality Q^2, the cross-section as a function of x_B has a a similar bump-like shape, which is explained by an interplay of two factors. For small $x_B \sim Q^2/2m_N E_e$ the elasticity y defined in (3) approaches one, which causes a suppression due to a prefactor in (1). In the opposite limit, the suppression $\sim (1-x)^n$ is due to the implemented parametrization of GPDs. Since the contribution of NLO terms is sizable, for its evaluation we use coefficient functions which account for NLO corrections. To estimate the uncertainty due to higher order corrections (represented by the green band), we varied the factorization scale μ_F in the range $\mu_F \in (Q/2,\, 2Q)$. As was discussed in Section II, the coefficient functions (9,11,14) have nonanalytic behavior $\sim \ln^2 v$ in the region of small-$v, \bar{v} = (\xi \pm x)/2\xi$, and therefore this region requires special attention. Physically, collinear factorization is not valid here and the transverse momenta of mesons become important. In order to assess the relative contribution of this region, we performed an evaluation with NLO corrections switched off in the range $|v| \lesssim l_{\pi,\perp}^2/Q^2$, where the average transverse momentum of the pion $l_{\pi,\perp} \approx 0.3 - 0.4\,\mathrm{GeV}$ was estimated from the pion charge form factor [64–66]. As we can see from a comparison of solid and dashed lines, the contribution of the small-$|v|$ region is quite small, and therefore we expect that collinear factorization should give a reliable estimate in the considered kinematics. In the rightmost pane of the Figure 5, we have shown the relative (dominant) contribution of the GPDs H^u, H^d to the total result. Contributions of helicity flip and gluon GPDs constitute a minor (∼10%) correction to the full cross-section.

The contribution of the asymptotic Bethe-Heitler mechanism introduced in Section III is shown in the left pane of the Figure 6. We can see that for 11 GeV electron beams, its contribution is small and does not exceed ~ 1 per cent. The smallness of the harmonics c_n, s_n is explained by the fact that the kinematic prefactor $\sim \left(Q^2/t\right)$ enhancement in JLAB kinematics is not sufficient to compensate the suppression $\sim \mathcal{O}\left(\alpha_{\mathrm{em}}\right)$. Though formally both the BH term (18) and interference term (24) lead to appearance of the harmonics $c_0, ..., c_2$, the contribution from the former is suppressed by an additional power of α_{em} and thus in JLAB kinematics the harmonics get a major

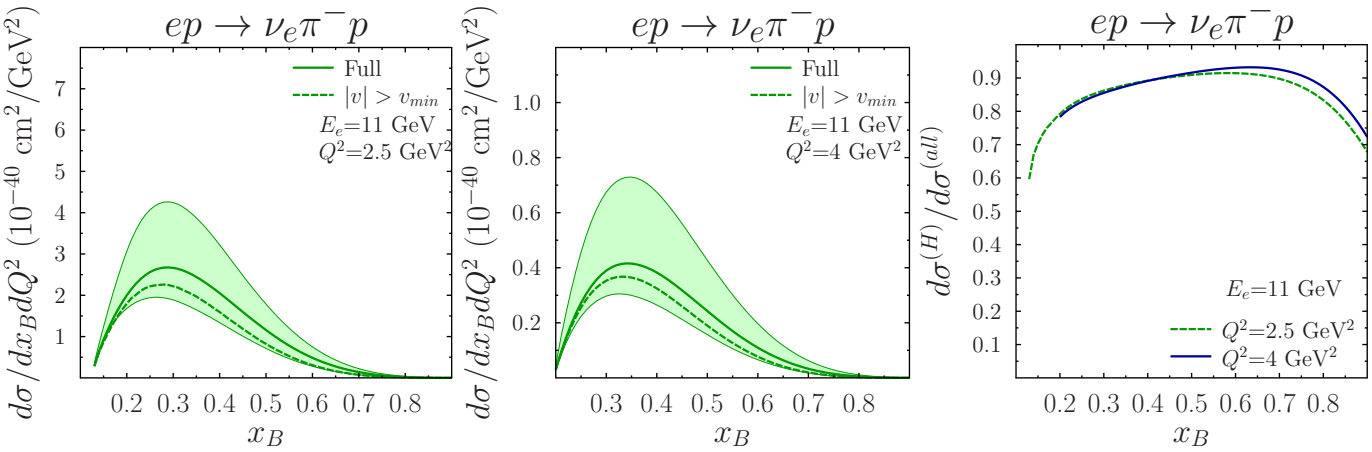

Figure 5: (color online) Left and central plots: Charged current pion production cross-section on a proton target at fixed electron energy, for virtualities Q^2=2.5 GeV^2(left) and Q^2=4 GeV^2(center) . Evaluations are performed using NLO coefficient functions, as discussed in Section II. The width of the band represents the uncertainty due to the factorization scale choice $\mu_F \in (Q/2, 2Q)$, as explained in the text. The dashed line corresponds to evaluation with omitted NLO corrections in the region of $x \approx \pm\xi$, where collinear factorization might give sizable corrections $\sim \mathcal{O}\left(l_\perp^2/Q^2\right)$. Right plot: Relative contribution of GPDs H^u, H^d to the total result.

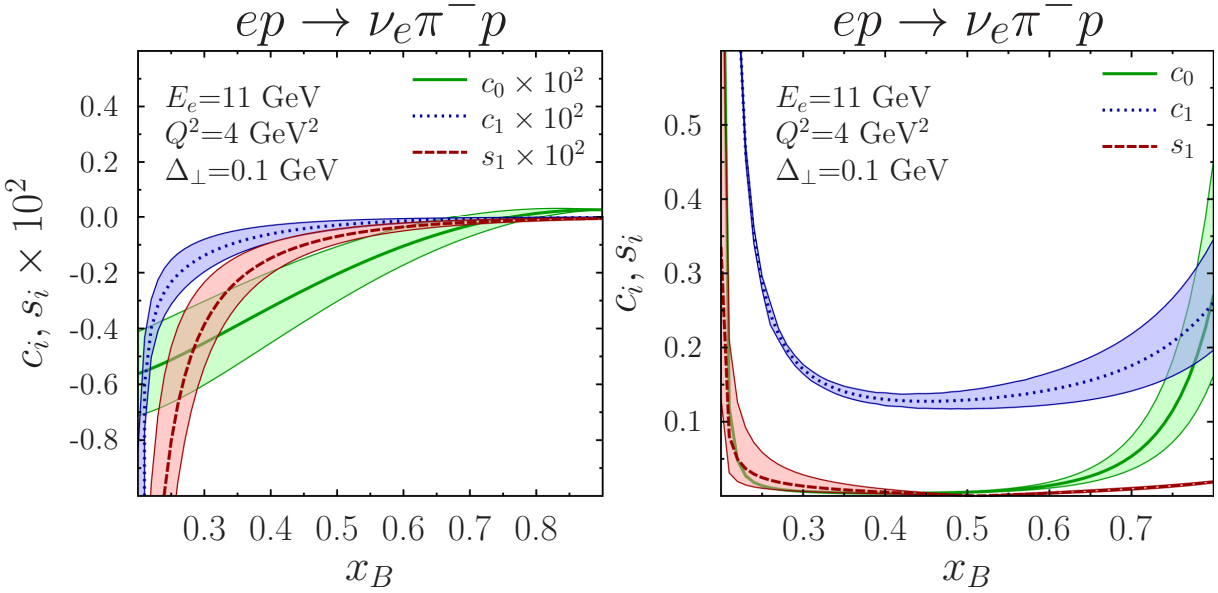

Figure 6: (color online) Left: Harmonics c_n, s_n in charged current pion production on a proton target, due to the interference with the Bethe-Heitler contribution. Right: Harmonics c_n, s_n generated due to twist-2 and twist-3 GPDs interference. In both plots the evaluations are performed using NLO coefficient functions, as discussed in Section II. The width of the band represents the uncertainty due to the factorization scale choice $\mu_F \in (Q/2, 2Q)$, as explained in the text.

contribution from the interference term. For the same reason, the harmonics c_2 (not shown in the plot) is extremely small: it gets contribution only from BH. In the right pane of the plot we have shown similar harmonics generated due to twist-three interference. The largest harmonics c_1 does not exceed 20 per cent and after averaging over the angle φ does not contribute to the total cross-section $d\sigma/dx_B dQ^2$. The harmonics c_0, which contributes to the integrated cross-section $d\sigma/dx_B dQ^2$ as a multiplicative factor $1 + c_0$, in the region of interest ($x_B \approx 0.4 \pm 0.2$) is small and constitutes a few percent correction.

For deeply virtual meson production in other channels the cross-section gets comparable contributions from GPDs of different partons. For this reason restrictions imposed by experimental data on GPDs of individual partons are less binding. Additionally, these channels present more challenges for experimental study. For example, for charged

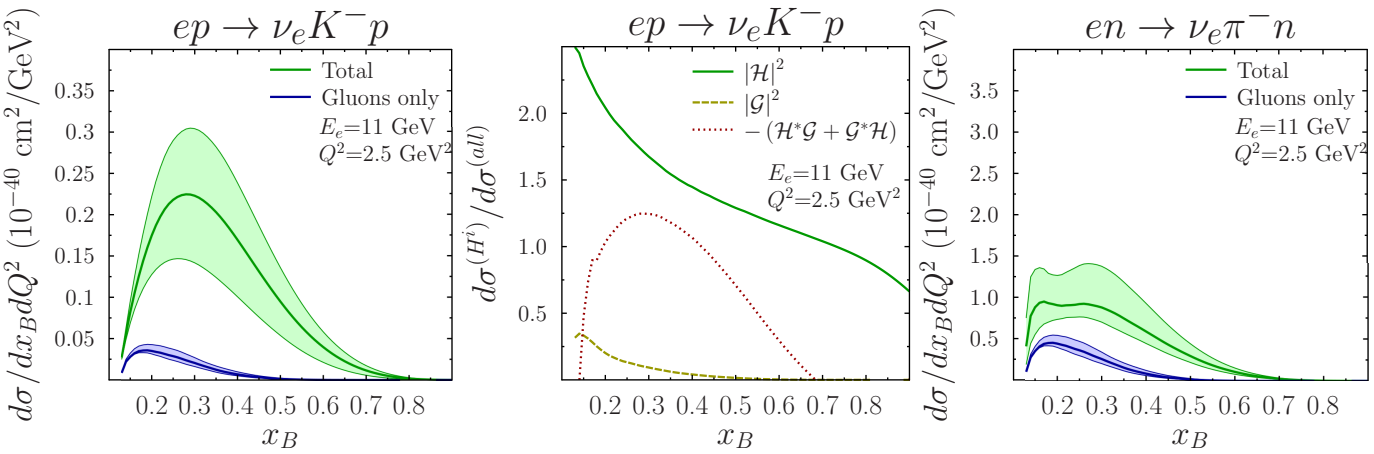

Figure 7: (color online) Left: Charged current kaon production cross-sections for fixed energy electron beam ($E_e \approx 11$ GeV). Central: relative fractions of different GPD components to the kaon production cross-section. We can see that the interference between quark and gluons is large and contributes with a negative sign. Right: Charged current pion production on a neutron target. In all plots the evaluations are performed using NLO coefficient functions, as discussed in Section II. The width of the band represents the uncertainty due to the factorization scale choice $\mu_F \in (Q/2, 2Q)$, as explained in the text.

current kaon production (see left pane in the Figure 7), we observe that the cross-section is small due to Cabibbo suppression ($\Delta S = 1$), so the statistical error will be larger. From the central pane in the Figure 7 we can see that the total cross-section of this process gets a sizable contribution from quark-gluon interference. Similarly, for charged current pion production on a neutron (right pane in the Figure 7), the cross-section gets significant contributions from gluon GPDs and its interference with quarks, and experimentally the precision will be affected by uncertainty in the reconstruction of scattered neutron kinematics.

For this reason we believe that the study of the GPDs with charged currents should be focused on the $ep \to \nu_e \pi^- p$ channel.

VI. KINEMATICS AND BACKGROUNDS

The reconstruction of the kinematics of the CCDVMP process $ep \to \nu_e\, \pi^- p$ presents certain challenges since it contains undetected neutruno in final state. From energy-momentum conservation

$$p_{\nu_e} = p_e + p_i - p_f - p_\pi, \tag{55}$$

where p_f and p_i are initial and final 4-momenta of the nucleon, p_e is the 4-momentum of the incident electron, and p_π is the 4-momentum of the produced pion, we may immediately get for the variables Q^2, x_B and t in the lab frame

$$Q^2 = 2\, m_N\, (E_f + E_\pi) - 2\, (E_f E_\pi - \vec{p}_f \cdot \vec{p}_\pi) - 2\, m_N^2 - m_\pi^2, \tag{56}$$

$$x_B = \frac{Q^2}{2 m_N\, \nu} = \frac{2\, m_N\, (E_f + E_\pi) - 2\, (E_f E_\pi - \vec{p}_f \cdot \vec{p}_\pi) - 2\, m_N^2 - m_\pi^2}{2 m_N\, (m_N + E_e - E_f - E_\pi)}, \tag{57}$$

$$t = \Delta^2 = (p_i - p_f)^2 = 2 m_N^2 - 2 m_N E_f. \tag{58}$$

We expect that sizeable backgrounds to the considered processes might come from the processes mediated by virtual photon, $ep \to e\, \pi^- p\, X$, where the scattered electron remains undetected. From charge conservation we conclude that the hadronic state (X) must include at least a charged pion, *i.e.* $e\, p \to e\, \pi^- \pi^+ p$ subprocess. In order to get rid of such backgrounds, we suggest to introduce a cutoff on the missing mass (mass of undetected neutrino),

$$p_\nu^2 \equiv m_{\nu_e}^2 = m_N^2 - Q^2 + 2 E_e\, (E_p + E_\pi - m_N) - 2\sqrt{E_e^2 - m_e^2}\, (p_{p,z} + p_{\pi,z})\,. \tag{59}$$

Current upper bounds on the mass of the neutrino m_{ν_e} are of order a few eV, however experimentally it is impossible to impose such cuts taking into account the precision available at JLAB. For this reason we suggest to use a more

relaxed cutoff

$$p_\nu^2 < m_\pi^2, \tag{60}$$

which is sufficient to get rid of any processes with production of additional (undetected) hadrons in photon-mediated processes.

Another possible source of backgrounds is due to misidentification of electron as pion in JLAB detectors, via $ep \to ep$ scattetring. However, contributions of such processes also might be eliminated. Let's consider the variable

$$\Delta E = E_e + m_N - E_{(\pi/e)} - E_f^* \tag{61}$$

where $E_{(\pi/e)}$ is the energy of the final pion or misidentified electron produced in the collision. In case of the process $ep \to ep$ the variable is exactly zero due to energy conservation, $\Delta E = 0$, whereas in case of the CCDVMP process $ep \to \nu_e\, \pi^- p$ the variable $\Delta E = E_\nu$ (neutrino energy). Imposing a cut

$$\Delta E \gtrsim 0.5\,\mathrm{GeV}, \tag{62}$$

we may completely eliminate this background. We analyzed all other possible background processes, yet we found that a combination of cuts (60,62) is sufficient to get rid of those contributions. For this reason we believe that the CCDVMP process might be measured in JLAB kinematics.

VII. CONCLUSIONS

In this paper we have shown that generalized parton distributions can be probed in charged current meson production processes, $ep \to \nu_e \pi^- p$. In contrast to pion *photo*production, these processes get a major contribution from the unpolarized GPDs H^u, H^d, and thus could be used to supplement studies of these GPDs in DVCS. The undetectability of the produced neutrino will not present major challenges for the kinematics reconstruction, since all final state hadrons are charged. We estimated the cross-sections in the kinematics of the upgraded 12 GeV Jefferson Laboratory experiments and found that thanks to the large luminosity, the process can be measured with reasonable statistics. We also estimated the contaminating contributions from the Bethe-Heitler mechanism and twist-three corrections due to transversity GPDs. We found that both are small, and for this reason the $ep \to \nu_e \pi^- p$ channel presents a clean probe of the target GPDs . If polarized targets become available in these experiments, it could enable to study various beam-target asymmetries, sensitive to the smaller GPDs E, $\tilde{H}$, $\tilde{E}$. We also demonstrated in Section VI that all photon-mediated backgrounds might be eliminated by additional cuts.

A code for the evaluation of the cross-sections, with various GPD models, is available on demand.

Acknowledgments

This research was partially supported by Proyecto Basal FB 0821 (Chile), the Fondecyt (Chile) grants 1140390 and 1140377, CONICYT (Chile) grant PIA ACT1413. Powered@NLHPC: This research was partially supported by the supercomputing infrastructure of the NLHPC (ECM-02). Also, we thank Yuri Ivanov for technical support of the USM HPC cluster where part of evaluations were done.

[1] X. D. Ji and J. Osborne, Phys. Rev. D **58** (1998) 094018 [arXiv:hep-ph/9801260].
[2] J. C. Collins and A. Freund, Phys. Rev. D **59**, 074009 (1999).
[3] R. Duprï¿œ, M. Guidal, S. Niccolai and M. Vanderhaeghen, arXiv:1704.07330 [hep-ph].
[4] D. Mueller, D. Robaschik, B. Geyer, F. M. Dittes and J. Horejsi, Fortsch. Phys. **42**, 101 (1994) [arXiv:hep-ph/9812448].
[5] X. D. Ji, Phys. Rev. D **55**, 7114 (1997).
[6] X. D. Ji, J. Phys. G **24**, 1181 (1998) [arXiv:hep-ph/9807358].
[7] A. V. Radyushkin, Phys. Lett. B **380**, 417 (1996) [arXiv:hep-ph/9604317].
[8] A. V. Radyushkin, Phys. Rev. D **56**, 5524 (1997).
[9] A. V. Radyushkin, arXiv:hep-ph/0101225.
[10] J. C. Collins, L. Frankfurt and M. Strikman, Phys. Rev. D **56**, 2982 (1997).
[11] S. J. Brodsky, L. Frankfurt, J. F. Gunion, A. H. Mueller and M. Strikman, Phys. Rev. D **50**, 3134 (1994).
[12] K. Goeke, M. V. Polyakov and M. Vanderhaeghen, Prog. Part. Nucl. Phys. **47**, 401 (2001) [arXiv:hep-ph/0106012].

[13] M. Diehl, T. Feldmann, R. Jakob and P. Kroll, Nucl. Phys. B **596**, 33 (2001) [Erratum-ibid. B **605**, 647 (2001)] [arXiv:hep-ph/0009255].
[14] A. V. Belitsky, D. Mueller and A. Kirchner, Nucl. Phys. B **629**, 323 (2002) [arXiv:hep-ph/0112108].
[15] M. Diehl, Phys. Rept. **388**, 41 (2003) [arXiv:hep-ph/0307382].
[16] A. V. Belitsky and A. V. Radyushkin, Phys. Rept. **418**, 1 (2005) [arXiv:hep-ph/0504030].
[17] V. Kubarovsky [CLAS Collaboration], Nucl. Phys. Proc. Suppl. **219-220**, 118 (2011).
[18] S. Ahmad, G. R. Goldstein and S. Liuti, Phys. Rev. D **79** (2009) 054014 [arXiv:0805.3568 [hep-ph]].
[19] S. V. Goloskokov and P. Kroll, Eur. Phys. J. C **65**, 137 (2010) [arXiv:0906.0460 [hep-ph]].
[20] S. V. Goloskokov and P. Kroll, Eur. Phys. J. A **47**, 112 (2011) [arXiv:1106.4897 [hep-ph]].
[21] G. R. Goldstein, J. O. G. Hernandez and S. Liuti, arXiv:1201.6088 [hep-ph].
[22] I. V. Anikin, D. Y. Ivanov, B. Pire, L. Szymanowski and S. Wallon, Nucl. Phys. B **828**, 1 (2010) [arXiv:0909.4090 [hep-ph]].
[23] M. Diehl, T. Gousset and B. Pire, Phys. Rev. D **59**, 034023 (1999) [hep-ph/9808479].
[24] L. Mankiewicz, G. Piller and A. Radyushkin, **10**, 307 (1999) [hep-ph/9812467].
[25] L. Mankiewicz and G. Piller, Phys. Rev. D **61**, 074013 (2000) [hep-ph/9905287].
[26] R. Boussarie, B. Pire, L. Szymanowski and S. Wallon, arXiv:1708.09164 [hep-ph].
[27] E. R. Berger, M. Diehl and B. Pire, Eur. Phys. J. C **23**, 675 (2002) [hep-ph/0110062].
[28] B. Pire, L. Szymanowski and J. Wagner, Phys. Rev. D **79**, 014010 (2009) [arXiv:0811.0321 [hep-ph]].
[29] M. Boï¿œr, M. Guidal and M. Vanderhaeghen, Eur. Phys. J. A **51**, no. 8, 103 (2015).
[30] D. Mueller, B. Pire, L. Szymanowski and J. Wagner, Phys. Rev. D **86**, 031502 (2012) [arXiv:1203.4392 [hep-ph]].
[31] T. Sawada, W. C. Chang, S. Kumano, J. C. Peng, S. Sawada and K. Tanaka, Phys. Rev. D **93**, no. 11, 114034 (2016) [arXiv:1605.00364 [nucl-ex]].
[32] D. Y. Ivanov, A. Schafer, L. Szymanowski and G. Krasnikov, Eur. Phys. J. C **34**, no. 3, 297 (2004) Erratum: [Eur. Phys. J. C **75**, no. 2, 75 (2015)] [hep-ph/0401131].
[33] D. Y. Ivanov, B. Pire, L. Szymanowski and J. Wagner, arXiv:1510.06710 [hep-ph].
[34] F. Gautheron *et al.* [COMPASS Collaboration], SPSC-P-340, CERN-SPSC-2010-014.
[35] O. Kouznetsov [COMPASS Collaboration], Nucl. Part. Phys. Proc. **270-272**, 36 (2016).
[36] A. Ferrero [COMPASS Collaboration], AIP Conf. Proc. **1523**, 75 (2012).
[37] A. Sandacz [COMPASS Collaboration], J. Phys. Conf. Ser. **678**, no. 1, 012045 (2016).
[38] A. Sandacz [COMPASS Collaboration], PoS QCDEV **2016**, 018 (2017).
[39] L. Silva, Few Body Syst. **54**, no. 7-10, 1075 (2013).
[40] P. Kroll, JPS Conf. Proc. **13**, 010014 (2017).
[41] B. Z. Kopeliovich, I. Schmidt and M. Siddikov, Phys. Rev. D **86** (2012), 113018 [arXiv:1210.4825 [hep-ph]].
[42] D. Drakoulakos *et al.* [Minerva Collaboration], hep-ex/0405002.
[43] B. Z. Kopeliovich, I. Schmidt and M. Siddikov, Phys. Rev. D **89**, no. 5, 053001 (2014) [arXiv:1401.1547 [hep-ph]].
[44] M. Siddikov and I. Schmidt, Phys. Rev. D **95**, no. 1, 013004 (2017) [arXiv:1611.07294 [hep-ph]].
[45] L. L. Frankfurt, P. V. Pobylitsa, M. V. Polyakov and M. Strikman, Phys. Rev. D **60** (1999) 014010 [hep-ph/9901429].
[46] B. Pire and L. Szymanowski, Phys. Rev. Lett. **115** (2015), 092001 [arXiv:1505.00917 [hep-ph]].
[47] B. Pire and L. Szymanowski, Acta Phys. Polon. Supp. **8**, 883 (2015) [arXiv:1510.01869 [hep-ph]].
[48] B. Pire, L. Szymanowski and J. Wagner, EPJ Web Conf. **112**, 01018 (2016) [arXiv:1601.07666 [hep-ph]].
[49] B. Pire, L. Szymanowski and J. Wagner, Phys. Rev. D **95**, no. 9, 094001 (2017) [arXiv:1702.00316 [hep-ph]].
[50] B. Pire, L. Szymanowski and J. Wagner, Phys. Rev. D **95**, no. 11, 114029 (2017) [arXiv:1705.11088 [hep-ph]].
[51] D. Androic *et al.* [Qweak Collaboration], Phys. Rev. Lett. **111** (2013) no.14, 141803 [arXiv:1307.5275 [nucl-ex]].
[52] J. Alcorn *et al.*, Nucl. Instrum. Meth. A **522**, 294 (2004).
[53] M. Vanderhaeghen, P. A. M. Guichon and M. Guidal, Phys. Rev. Lett. **80**, 5064 (1998).
[54] S. V. Goloskokov and P. Kroll, Eur. Phys. J. C **50**, 829 (2007) [hep-ph/0611290].
[55] S. V. Goloskokov and P. Kroll, Eur. Phys. J. C **53**, 367 (2008) [arXiv:0708.3569 [hep-ph]].
[56] S. V. Goloskokov and P. Kroll, Eur. Phys. J. C **59** (2009) 809 [arXiv:0809.4126 [hep-ph]].
[57] B. Z. Kopeliovich, Ivï¿œn Schmidt and M. Siddikov, Nucl. Phys. A **918**, 41 (2013) [arXiv:1108.5654 [hep-ph]].
[58] A. V. Belitsky and D. Mueller, Phys. Lett. B **513**, 349 (2001) [hep-ph/0105046].
[59] D. Y. Ivanov, L. Szymanowski and G. Krasnikov, JETP Lett. **80**, 226 (2004) [Pisma Zh. Eksp. Teor. Fiz. **80**, 255 (2004)] Erratum: [JETP Lett. **101**, no. 12, 844 (2015)] , [hep-ph/0407207].
[60] M. Diehl and W. Kugler, Eur. Phys. J. C **52**, 933 (2007) [arXiv:0708.1121 [hep-ph]].
[61] E. Braaten and S. M. Tse, Phys. Rev. D **35**, 2255 (1987).
[62] B. Melic, B. Nizic and K.˜Passek, Phys. Rev. **60**, 074004 (1999) [hep-ph/9802204].
[63] B. Z. Kopeliovich, I. Schmidt and M. Siddikov, Phys. Rev. D **87**, 033008 (2013) [arXiv:1301.7014 [hep-ph]].
[64] S. R. Amendolia *et al.*, Phys. Lett. **146B** (1984) 116.
[65] E. B. Dally *et al.*, Phys. Rev. Lett. **48**, 375 (1982).
[66] F. Schlumpf, Phys. Rev. D **50**, 6895 (1994) [hep-ph/9406267].